

RESEARCH ARTICLE

# Effects of Hormone Therapy on Brain Volumes Changes of Postmenopausal Women Revealed by Optimally-Discriminative Voxel-Based Morphometry

Tianhao Zhang<sup>1\*</sup>, Ramon Casanova<sup>2</sup>, Susan M. Resnick<sup>3</sup>, JoAnn E. Manson<sup>4,5</sup>, Laura D. Baker<sup>6</sup>, Claudia B. Padual<sup>7,8</sup>, Lewis H. Kuller<sup>9</sup>, R. Nick Bryan<sup>1</sup>, Mark A. Espeland<sup>2</sup>, Christos Davatzikos<sup>1</sup>

**1** Center for Biomedical Image Computing and Analytics, Department of Radiology, University of Pennsylvania, Philadelphia, Pennsylvania, United States of America, **2** Department of Biostatistical Sciences, Wake Forest School of Medicine, Winston-Salem, North Carolina, United States of America, **3** Laboratory of Behavioral Neuroscience, National Institute on Aging, Baltimore, Maryland, United States of America, **4** Division of Preventive Medicine, Department of Medicine, Brigham and Women's Hospital and Harvard Medical School, Boston, Massachusetts, United States of America, **5** Department of Epidemiology, Harvard School of Public Health, Boston, Massachusetts, United States of America, **6** Department of Internal Medicine and Epidemiology, Wake Forest School of Medicine, Winston-Salem, North Carolina, United States of America, **7** Sierra Pacific Mental Illness Research, Education and Clinical Center, VA Palo Alto Health Care System, Palo Alto, California, United States of America, **8** Department of Psychiatry and Behavioral Sciences, Stanford University, Stanford, California, United States of America, **9** Department of Epidemiology, Graduate School of Public Health, University of Pittsburgh, Pittsburgh, Pennsylvania, United States of America

\* [tianhao.zhang@uphs.upenn.edu](mailto:tianhao.zhang@uphs.upenn.edu)



**OPEN ACCESS**

**Citation:** Zhang T, Casanova R, Resnick SM, Manson JE, Baker LD, Padual CB, et al. (2016) Effects of Hormone Therapy on Brain Volumes Changes of Postmenopausal Women Revealed by Optimally-Discriminative Voxel-Based Morphometry. PLoS ONE 11(3): e0150834. doi:10.1371/journal.pone.0150834

**Editor:** Angel Alberich-Bayarri, Le Fe Health Research Institute, SPAIN

**Received:** August 31, 2015

**Accepted:** February 20, 2016

**Published:** March 14, 2016

**Copyright:** This is an open access article, free of all copyright, and may be freely reproduced, distributed, transmitted, modified, built upon, or otherwise used by anyone for any lawful purpose. The work is made available under the [Creative Commons CC0](https://creativecommons.org/licenses/by/4.0/) public domain dedication.

**Data Availability Statement:** Data are available from Women's Health Initiative (WHI). WHI regularly releases the data to public through the Biologic Specimen and Data Repository Information Coordinating Center (BioLINCC, <https://biolincc.nhlbi.nih.gov/home/>) for researchers who meet the criteria for access to the data. Researchers seeking data which are not currently under public release should get approval from the WHI Publications & Presentations committee and place a signed data release agreement with WHI Clinical Coordinating

## Abstract

### Backgrounds

The Women's Health Initiative Memory Study Magnetic Resonance Imaging (WHIMS-MRI) provides an opportunity to evaluate how menopausal hormone therapy (HT) affects the structure of older women's brains. Our earlier work based on region of interest (ROI) analysis demonstrated potential structural changes underlying adverse effects of HT on cognition. However, the ROI-based analysis is limited in statistical power and precision, and cannot provide fine-grained mapping of whole-brain changes.

### Methods

We aimed to identify local structural differences between HT and placebo groups from WHIMS-MRI in a whole-brain refined level, by using a novel method, named Optimally-Discriminative Voxel-Based Analysis (ODVBA). ODVBA is a recently proposed imaging pattern analysis approach for group comparisons utilizing a spatially adaptive analysis scheme to accurately locate areas of group differences, thereby providing superior sensitivity and specificity to detect the structural brain changes over conventional methods.

### Results

Women assigned to HT treatments had significant Gray Matter (GM) losses compared to the placebo groups in the anterior cingulate and the adjacent medial frontal gyrus, and the

Center (fax: 206-667-4142; email: [helpdesk@whi.org](mailto:helpdesk@whi.org)).

**Funding:** The WHI program is funded by the National Heart, Lung, and Blood Institute (<http://www.nhlbi.nih.gov/>), National Institutes of Health, U.S. Department of Health and Human Services through contracts HHSN268201100046C, HHSN268201100001C, HHSN268201100002C, HHSN268201100003C, HHSN268201100004C, and HHSN271201100004C. TZ and CD were supported by NIH grant R01AG14971. The funders had no role in study design, data collection and analysis, decision to publish, or preparation of the manuscript.

**Competing Interests:** The authors have declared that no competing interests exist.

orbitofrontal cortex, which persisted after multiple comparison corrections. There were no regions where HT was significantly associated with larger volumes compared to placebo, although a trend of marginal significance was found in the posterior cingulate cortical area. The CEE-Alone and CEE+MPA groups, although compared with different placebo controls, demonstrated similar effects according to the spatial patterns of structural changes.

## Conclusions

HT had adverse effects on GM volumes and risk for cognitive impairment and dementia in older women. These findings advanced our understanding of the neurobiological underpinnings of HT effects.

## Introduction

The Women's Health Initiative Memory Study (WHIMS) provided a unique opportunity for researchers to examine critical questions regarding the effects of hormone therapy (HT) on brain structure of postmenopausal women. Results from the WHIMS study [1, 2, 3, 4] indicated that conjugated equine estrogens, with and without progestin, increase the risk of dementia and have adverse effects on cognition in women aged 65 and over.

Advances in Magnetic Resonance Imaging (MRI) make it possible to non-invasively and sensitively measure pathologic changes in cortical and subcortical brain parenchyma. WHIMS-MRI, as a sub-study of the Women's Health Initiative (WHI) and WHIMS, was able to provide a comprehensive examination of the effects of hormone therapy on regional brain structure in postmenopausal women. In our earlier work [5], we investigated whether regions of interest (ROI) including total brain, hippocampus, frontal lobe, and others labeled on MRI scans acquired post-trial, show significant differences in volumes for older women who had been assigned to HT compared with those assigned to placebo. The results suggested that women assigned to HT had decreased volumes in specific regions compared with those assigned to placebo, offering a potential mechanism underlying the adverse effects of HT on cognition. However, the ROI-based analysis may lack statistical precision as it does not take into account the complex and anisotropic structural information circumscribed by the brain ROIs. Moreover, the outputs of the ROI analysis can only provide gross information on volumetric structure of particular regions, which cannot meet the current need of fine-grained mapping of brain alterations.

The current study aimed to identify local structural differences between HT and placebo groups from WHIMS-MRI, using a voxel-wise method, which analyzes the whole brain automatically, resulting in a brain map that reflects statistical significance on a refined level. Voxel-Based Morphometry (VBM) [6, 7, 8] is one such technique, commonly used in past years for mapping neuroanatomical differences including those associated with HT [9, 10, 11]. However, the conventional VBM method has technical shortcomings. First, the general linear model (GLM [12]) exploited in VBM has limited statistical power due to its mass-univariate nature that discards complex multivariate relationships in the data [13]. Second, the Gaussian smoothing, typically applied prior to the GLM step in VBM, has been shown to increase the risk of both false positive and false negative results [14, 15, 16] due to its blurring effects on the spatial signals of images.

In this study we used a novel method, termed optimally-discriminative voxel-based analysis (ODVBA), which is a recently proposed imaging pattern analysis approach for group

comparisons recently proposed by [17, 18]. ODVBA utilizes a spatially adaptive analysis scheme to accurately locate areas of group differences, and thereby transcends the limitations of the commonly used Gaussian smoothing with a fixed kernel size that precedes GLM, translating to superior sensitivity and specificity to detect the structural brain changes. The performance of ODVBA has been extensively validated in both the simulated data in which the ground truth on the simulated abnormalities is known [17] and the real data from clinical studies in Alzheimer's Disease [17, 18], schizophrenia [18, 19], ADHD [20], imaging effects of diabetes [21], among others. To our knowledge, the present study is the first voxel-based morphometric study to investigate the structural brain changes associated with hormone therapy in the WHIMS project.

## Materials and Methods

### Participants

As an ancillary study of WHI (registered at [ClinicalTrials.gov](https://clinicaltrials.gov) with ID# NCT00000611), WHIMS was conducted to investigate the effects of hormone therapy on risk of dementia and changes in cognitive function in women aged 65 or older. Data are available from Women's Health Initiative ([www.whi.org](http://www.whi.org)), once a signed data use agreement is in place. For more details refer to the associated Data Availability statement. The subjects were randomized into the parallel placebo-controlled randomized clinical trials of 0.625 mg/d conjugated equine estrogens (CEE) therapy alone (CEE-Alone) and in combination with 2.5 mg/d medroxyprogesterone acetate (CEE+MPA). The study protocols and consent forms were approved by National Institutes of Health and Institutional Review Boards of all 40 participating clinical centers (<https://www.nhlbi.nih.gov/whi/ccenterlist.htm>). Written informed consent was obtained from each participant. Participant records/information was anonymized and de-identified prior to analysis. The details of this study were previously published [1, 2, 22].

The WHIMS-MRI trial, conducted at 14 of 39 WHIMS sites [5, 23], was designed to determine whether ischemic lesion volumes and volumes of brain parenchyma differed between women previously randomized to CEE-Alone and CEE+MPA and their respective placebo groups. For the overall with trial, randomization was stratified by site to achieve balance. Among participants included in our analysis, treatment assignments were balanced among clinics ( $p = 0.32$ ). The recruitment started in January 2005 and ended in April 2006, approximately 1.4 years for CEE-Alone and 3.0 years for CEE+MPA after the termination of the WHI trial. Of the total sample of 1424 participants who completed the scanning, 1,365 participants who met the reading criteria were included in this analysis, including 254 active and 256 placebo participants in the CEE-Alone trial, and 420 active and 435 placebo participants in the CEE+MPA trial, making the total 674 HT and 691 placebo participants. The demographic, life-style, and clinical characteristics of the women included in this study are listed in [Table 1](#). As demonstrated, there were no marked differences in the related risk factors between the active treatment groups and the associated placebo.

### Image Acquisition and Pre-Processing

MRI scans were performed using a standardized protocol which was developed by investigators at the MRI Quality Control (QC) Center in the Department of Radiology of University of Pennsylvania (UPenn). The scanners were standardized by American College of Radiology (ACR) phantom QC protocol as follows. Before each clinical site can enroll subjects into WHIMS study protocol, a set of test scans on the ACR QC phantoms [24] and a volunteer have been submitted for review and approved by the MRI QC Center in UPenn. The ACR phantom tests have been performed on a quarterly basis. Details on procedures for acquisition

**Table 1. Demographic, lifestyle, and clinical characteristics of WHIMS-MRI women by treatment assignment.**

Variable	WHIMS-MRI: CEE-Alone		WHIMS-MRI: CEE+MPA		Statistics ( <i>p</i> values, %)		
	CEE-Alone (n = 254)	Placebo (n = 256)	CEE+MPA (n = 420)	Placebo (n = 435)	CEE-Alone vs. Placebo	CEE+MPA vs. Placebo	HT vs. Placebo
<b>Age, no. (%)</b>					90.82	87.94	87.33
65–69 y	123(48.43)	128(50.00)	220 (52.38)	225 (51.72)			
70–74 y	93(36.61)	89 (34.77)	147 (35.00)	150 (34.48)			
75 + y	38 (14.96)	39 (15.23)	53 (12.62)	60 (13.79)			
<b>Ethnicity</b>					9.63	27.65	97.32
Black/African American	13 (5.16)	16 (6.27)	17 (4.05)	15 (3.46)			
White, non-Hispanic	222 (88.10)	232(90.98)	392 (93.33)	399 (91.94)			
Other	17 (6.75)	7 (2.75)	11 (2.62)	22 (4.61)			
<b>Education</b>					13.05	51.59	94.43
<High school	16 (6.30)	8 (3.13)	15 (3.58)	21 (4.85)			
High school /GED	69 (27.17)	69 (26.95)	84 (20.05)	95 (21.94)			
>High school, <4 y college	94 (37.10)	115 (44.92)	174 (41.53)	161 (37.18)			
>4 y college	75 (29.53)	64 (25.00)	146 (34.84)	156 (36.03)			
<b>Smoking Status</b>					44.90	63.60	69.82
Never	147 (58.57)	142 (55.69)	248 (59.33)	247 (57.44)			
Former	95 (37.85)	98 (38.43)	152 (36.36)	168 (39.07)			
Current	9 (3.59)	15 (5.88)	18 (4.31)	15 (3.49)			
<b>Body Mass Index</b>					77.45	69.06	73.06
<25 kg/m <sup>2</sup>	59 (23.41)	63 (24.71)	134 (31.98)	153 (35.25)			
25–29 kg/m <sup>2</sup>	98 (38.89)	107 (41.96)	157 (37.47)	151 (34.79)			
30–34 kg/m <sup>2</sup>	60 (23.81)	55 (21.57)	89 (21.24)	86 (19.82)			
≥35 kg/m <sup>2</sup>	35 (13.89)	30 (11.76)	39 (9.31)	44 (10.14)			
<b>Hypertension Status</b>					38.11	24.42	68.68
None	120 (47.24)	134 (52.34)	227 (54.05)	234 (53.79)			
Current/controlled	51 (20.08)	53 (20.70)	53 (12.62)	45 (10.34)			
Current/uncontrolled	83 (32.68)	69 (26.95)	140 (33.33)	156 (35.86)			
<b>Prior Cardiovascular Disease</b>					92.22	20.95	36.59
No	233 (91.73)	233 (91.02)	399 (95.00)	414 (95.17)			
History of stroke	3 (1.18)	4 (1.56)	1 (0.24)	5 (1.15)			
History of other CVD	18 (7.09)	19 (7.42)	20 (4.76)	16 (3.68)			
<b>Diabetes</b>					49.72	36.05	22.47
No	238 (93.70)	235 (91.80)	405 (96.43)	414 (95.17)			
Yes	16 (6.30)	21 (8.20)	15 (3.57)	21 (4.83)			
<b>Prior Hormone Therapy</b>					59.56	70.42	58.78
No	129 (50.79)	124 (48.44)	328 (78.10)	335 (77.01)			
Yes	125 (49.21)	132 (51.56)	92 (21.90)	100 (22.99)			
<b>3MS score</b>					77.10	46.60	38.40
<90	20 (7.94)	19 (7.48)	20 (4.77)	17 (3.96)			
90–94	50 (19.84)	57 (22.44)	63 (15.04)	77 (17.95)			
95–100	182 (74.22)	178 (70.08)	336 (80.19)	335 (78.09)			

doi:10.1371/journal.pone.0150834.t001

and processing were provided previously [5, 25]. Briefly, the scans were obtained with a field of view = 22 cm and a matrix of 256×256. Included were oblique axial spin density/T2-weighted spin echo (TR:3200 ms, TE = 30/120 ms, slice thickness = 3 mm), fluid-attenuated inversion recovery (FLAIR) T2-weighted spin echo (TR = 8000 ms, TI = 2000 ms, TE = 100 ms, slice thickness = 3 mm), and oblique axial three-dimensional T1-weighted gradient echo (flip angle = 30 degrees, TR = 21 ms, TE = 8 ms, slice thickness = 1.5 mm) images from the vertex to the skull base parallel to the anterior commissure–posterior commissure (AC-PC) plane.

The T1-weighted images were preprocessed according to a number of steps including 1) alignment of the brain with the AC-PC plane by manually; 2) removal of extra-cranial material using the BET method [26]; 3) tissue segmentation into gray matter (GM), white matter (WM), and cerebrospinal fluid (CSF), using a method described in [27]; 4) high-dimensional image warping to a standard MNI space [28], through an elastic registration method [29]; 5) applying the deformation field that resulted from the spatial registration to the segmented images, thereby generating mass-preserved volumetric maps (or tissue density maps), named Regional Analysis of Volumes Examined in Normalized Space (RAVENS) maps (Davatzikos et al., 2001); and 6) correction for the effects of i) intracranial volume (ICV), ii) age, iii) clinic site, and iv) time from randomization to scan, using the multiple linear regression model [30].

## Statistical Analysis

Group comparisons were performed via voxel-based statistical analysis of the volumetric measurements by using ODVBA. The ODVBA software is freely available (<https://www.cbica.upenn.edu/sbia/software/odvba/>) under a BSD-style open source license. ODVBA is a recently proposed imaging pattern analysis framework used to more accurately detect the group differences in brain imaging data. ODVBA starts with the regional multivariate discriminative analyses with a non-negativity constraint, as an optimal anisotropic filtering of images that enhances group differences. Next, the whole brain map of statistic is calculated by tallying the weights of each voxel to all of the neighborhoods in which it belongs. Finally, the statistical significance maps are obtained via nonparametric permutation testing [31]: assuming that the null hypothesis is that there is no difference between two groups, the  $p$  value of each voxel is calculated by comparing the observed statistic to the random permutation distribution. The current study used 2,000 permutations to derive the significances.

To address the multiple-comparison problem, we implemented cluster-wise Family Wise Error (FWE) correction based on non-parametric permutation tests [31, 32, 33]. The cluster-wise FWE is reported to be more powerful [32] than the voxel-wise False Discovery Rate (FDR) correction [34, 35], because it takes into account the spatial correlations [33] within regional volumes. The resulting maps of significance were partitioned and analyzed according to the Automated Anatomical Labeling (AAL) package [36]. On each anatomical region, we calculated the cluster size, the  $t$  statistic (based on the means of the tissue density of the detected area per region, as well as in [17]), and the Talairach coordinate of the mass's center [37].

## Results

### GM Findings

**HT, CEE-Alone, and CEE+MPA < Placebo.** As shown in Fig 1 and Table 2, women assigned to HT (both CEE-Alone and CEE+MPA users) showed significantly less GM compared to those assigned to placebo in the medial prefrontal regions, including the bilateral anterior cingulate cortex ( $p < 0.05$ , FWE corrected) and the adjacent bilateral superior frontal gyrus ( $p < 0.05$ , FWE corrected) as well as the bilateral middle cingulate cortex ( $p < 0.05$ , FWE

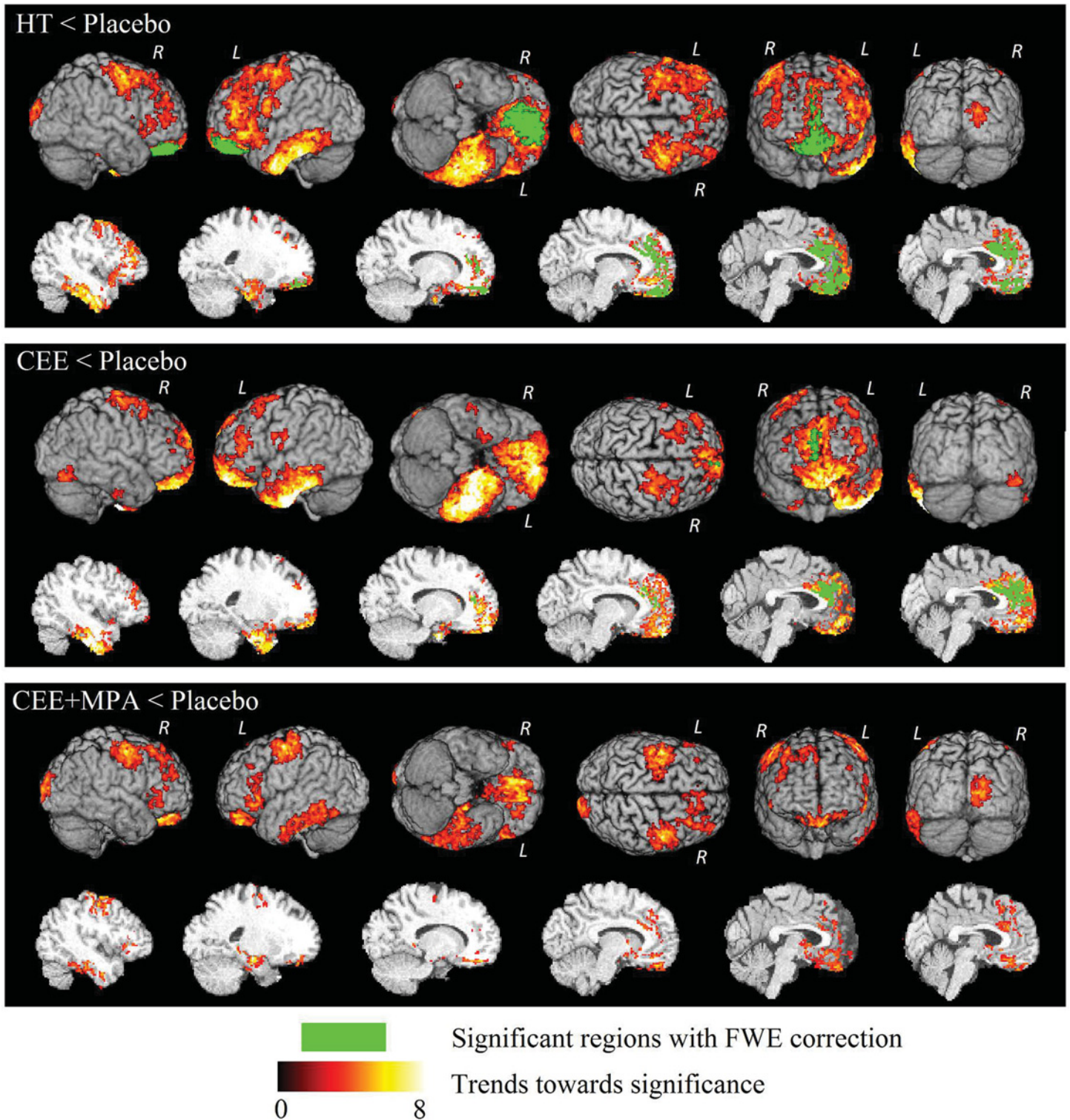


**Fig 1. 3D surface renderings (upper six images) and representative slices (lower six images) of the ODVBA results on GM volumes comparisons of HT groups < Placebo.** Green indicates the detected significant regions with FWE corrected  $p < 0.05$ ; regions of hot colors indicate the trends (uncorrected  $p < 0.05$ ) towards significance characterized by the  $-\log(p)$  values shown in the colorbar.

doi:10.1371/journal.pone.0150834.g001

**Table 2. The results of GM volume comparisons of HT groups < Placebo. N denotes the number of significant voxels in each anatomical region. t denotes the t value calculated.**

Comparisons	Methods	Anatomical Regions	Side	Talairach coordinates			N	t
				x	y	z		
<b>HT &lt; Placebo</b>	FWE( $p < .05$ )	Anterior Cingulate Cortex	L	-3.96	35.70	14.79	651	4.74
		Medial Superior Frontal Gyrus	L	-3.96	40.13	25.63	449	6.21
		Orbitofrontal Cortex	L	-3.96	49.96	-10.91	448	4.21
		Gyrus Rectus	L	-1.98	39.85	-18.82	333	3.98
		Gyrus Rectus	R	5.94	35.97	-18.62	186	4.89
		Anterior Cingulate Cortex	R	5.94	33.86	16.73	169	4.86
		Orbitofrontal Cortex	R	15.84	37.83	-20.40	95	3.80
		Middle Cingulate Cortex	R	5.94	28.60	28.05	49	2.98
		Middle Cingulate Cortex	L	-3.96	22.88	30.17	25	2.57
		Superior Frontal Gyrus	L	-11.88	28.87	33.56	11	2.84
		<b>CEE-Alone &lt; Placebo</b>	FWE( $p < .05$ )	Anterior Cingulate Cortex	L	-3.96	33.77	14.89
Medial Superior Frontal Gyrus	L			-1.98	43.82	21.76	329	5.64
Anterior Cingulate Cortex	R			5.94	37.55	12.86	204	5.74
Medial Superior Frontal Gyrus	R			5.94	50.56	1.15	79	4.12
Middle Cingulate Cortex	R			7.92	34.41	27.75	14	3.51

doi:10.1371/journal.pone.0150834.t002

corrected), and in the ventromedial prefrontal regions including the orbitofrontal cortex (bilateral:  $p < 0.05$ , FWE corrected) and the gyrus rectus (bilateral:  $p < 0.05$ , FWE corrected).

The comparison between CEE-Alone treated women and their respective placebo group revealed significantly lower GM volumes in the CEE-Alone group, which were predominantly located in the bilateral anterior cingulate cortex ( $p < 0.05$ , FWE corrected), the bilateral medial part of the superior frontal gyrus ( $p < 0.05$ , FWE corrected).

The CEE+MPA group did not show regions of significantly decreased GM volumes with multiple comparison correction, relative to the matched placebo, but did demonstrate trends toward lower volumes with a liberal uncorrected significance level (S1 Table) in the prefrontal cortex, in accord with the findings in the previous two comparisons. Moreover, all three comparisons revealed trend level volume reductions in left-sided temporal lobe structures (as shown in Fig 1 and S1 Table), including inferior temporal gyrus, parahippocampal gyrus, hippocampus, etc.

**HT, CEE-Alone, CEE+MPA > Placebo.** There were no significant differences indicative of greater volumes associated with HT surviving the multiple-comparison corrections, but three comparisons showed trends (Fig 2, S1 Table) for the parietal/occipital area, including the right calcarine, the right precuneus, and the left middle occipital gyrus.

### WM Findings

Analysis of local WM volumes revealed no significant differences after multiple comparison correction when comparisons were performed between HT, CEE-Alone, CEE+MPA and the respective placebo groups. However, as demonstrated in Fig 3 and S2 Table, we detected trends that were generally consistent with our findings in GM. Specifically, all three comparisons of HT, CEE-Alone, and CEE+MPA < Placebo showed consistently lower HT-associated WM volumes in regions around the bilateral medial frontal lobe, the bilateral orbitofrontal cortex, and the left temporal lobe. We also found trends toward greater HT-associated WM for all three comparisons for the parietal/occipital area.

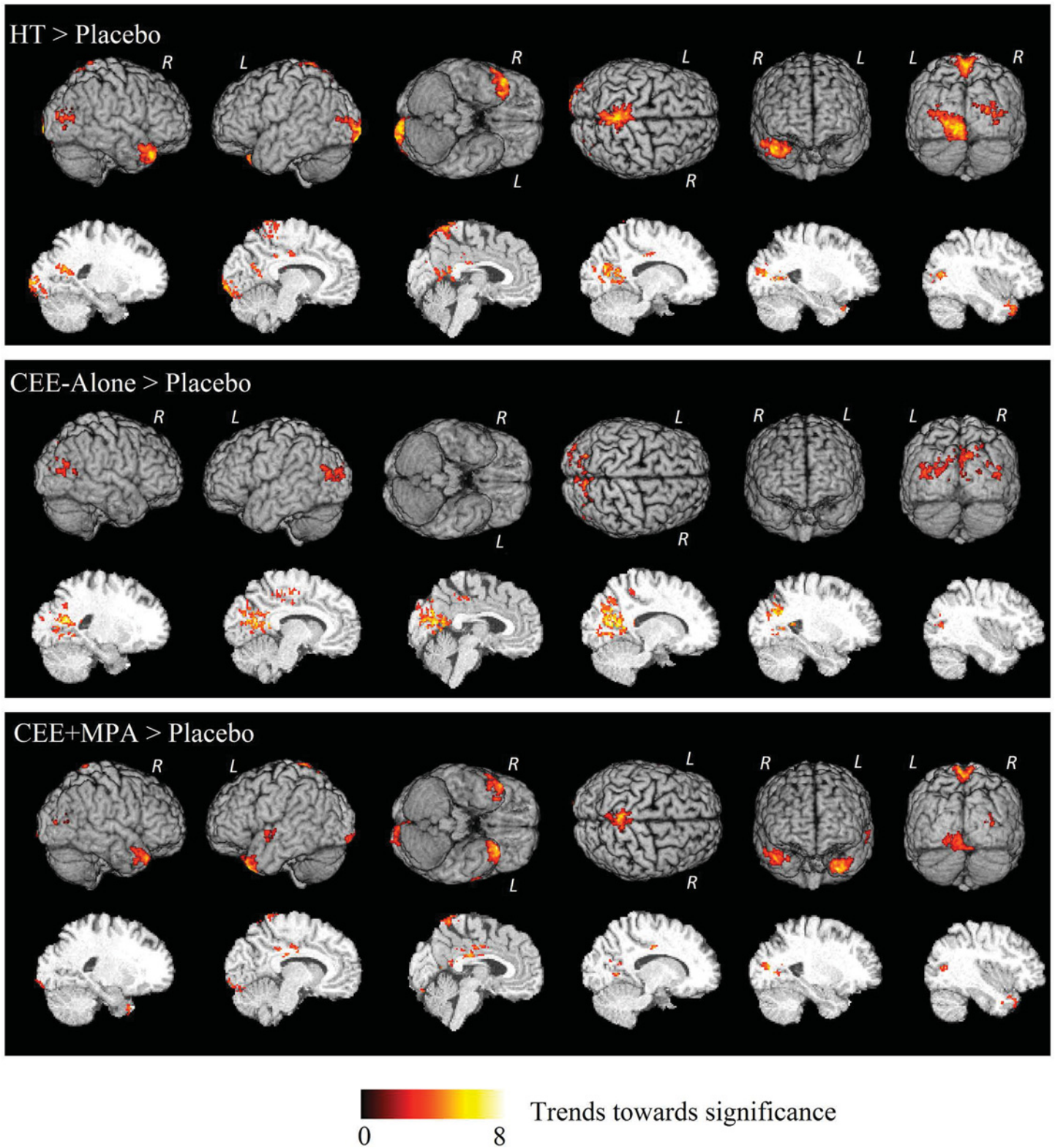


**Fig 2. 3D surface renderings (upper six images) and representative slices (lower six images) of the ODVBA results on GM volume comparisons of HT groups > Placebo.** Regions of hot colors indicate trends (uncorrected  $p < 0.05$ ) towards significance characterized by the  $-\log(p)$  values shown in the colorbar.

doi:10.1371/journal.pone.0150834.g002

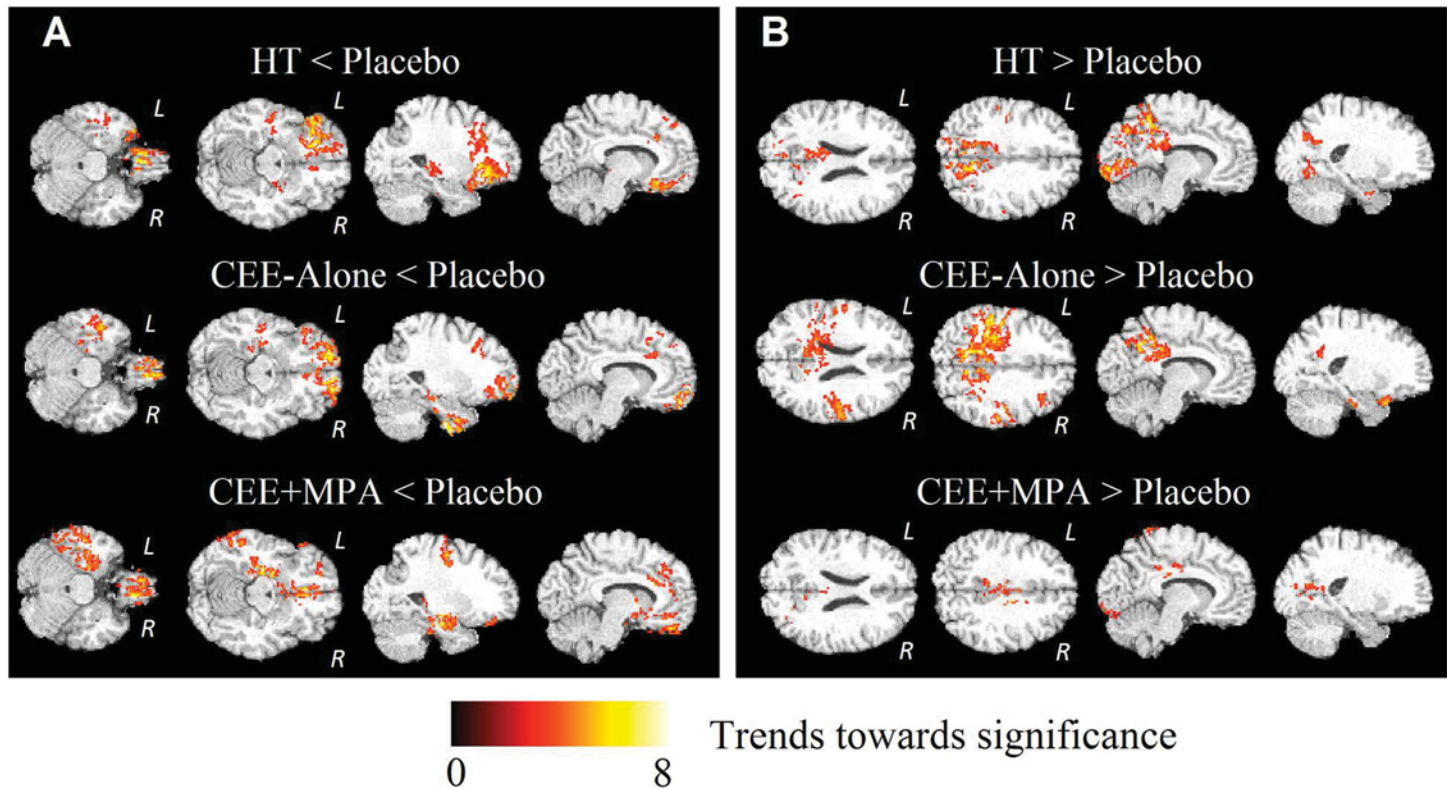


**Fig 3.** Representative slices of the ODBVA results on WM volume comparisons of (A) HT groups < Placebo, and (B) HT groups > Placebo. Regions of hot colors indicate trends (uncorrected  $p < 0.05$ ) towards significance characterized by the  $-\log(p)$  values shown in the colorbar.

doi:10.1371/journal.pone.0150834.g003

### Other Analyses

**CEE-Alone versus CEE+MPA.** CEE-Alone and CEE+MPA groups cannot be contrasted directly due to differences in their demographic and medical characteristics, requiring separate placebo groups for the two trials. In Fig 4, we demonstrate the overlap of significant findings for GM and WM (regions in red).

**Sensitivity analysis.** As women with other vulnerabilities may be more sensitive to the effects of HT, we recalculated outcomes by excluding women with low baseline cognition (3MS score < 90; 20 CEE subjects and 19 associated placebo; 20 CEE+MPA subjects and 17 associated placebo) and with diabetes (16 CEE subjects and 21 associated placebo; 15 CEE+MPA subjects and 21 associated placebo), which are with small numbers though. This can be regarded as a kind of sensitivity analysis that generally investigates how the uncertainty in the output of a model or system can be distributed to different sources of inputs [38]. The results indicated that the group analyses excluding women with these vulnerabilities yielded the nearly the same patterns with those of the original analyses.

### Discussions

In WHIMS-MRI, we assessed the effects of postmenopausal HT on localized brain volume changes in a large sample of older women in the context of the WHI randomized clinical trials. Women had been previously assigned to either CEE-Alone or CEE+MPA and their respective placebos, allowing investigation of effects of postmenopausal hormone therapy using a novel voxel-based morphometric method to investigate effects across the entire brain. These analyses

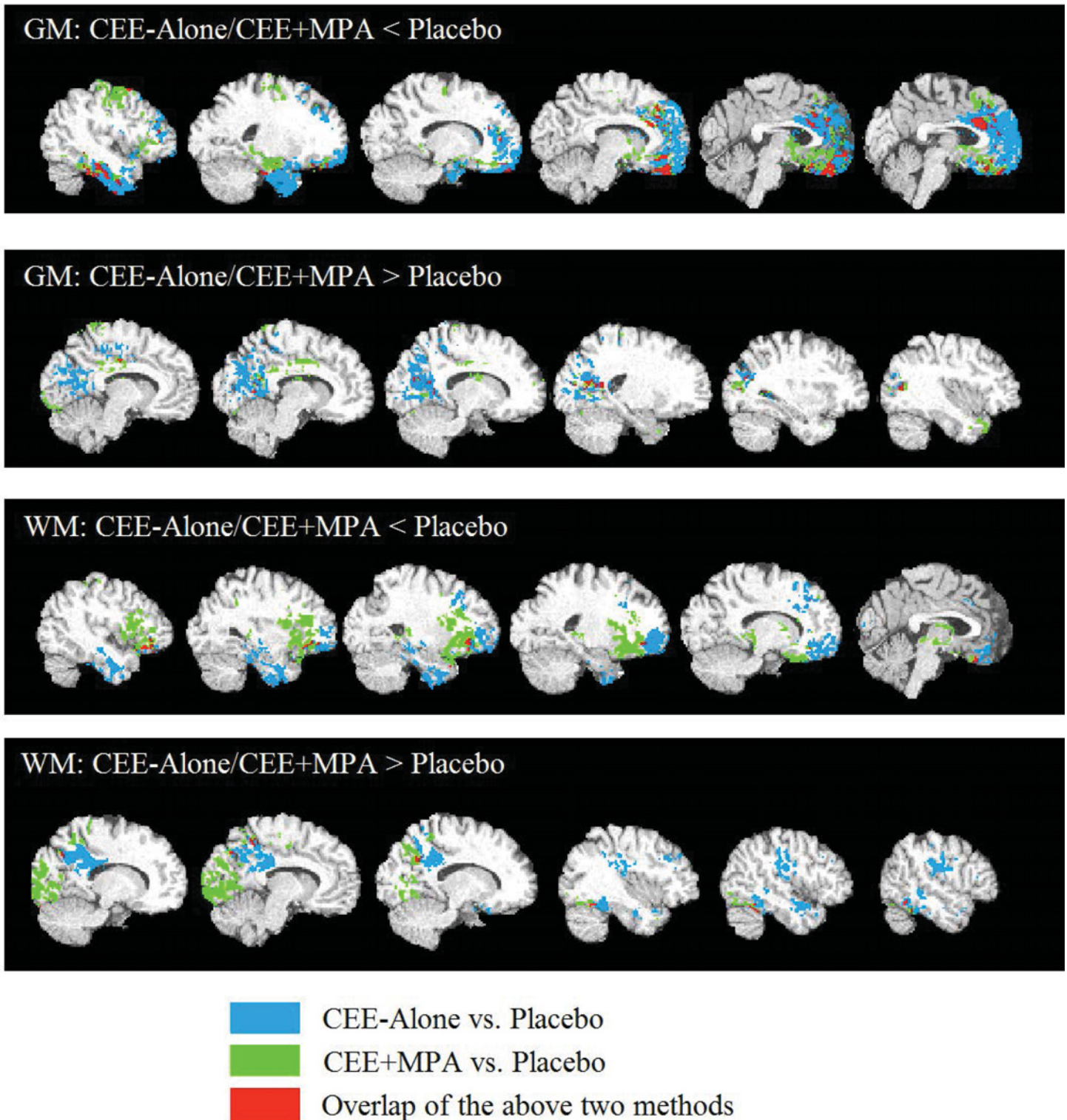


**Fig 4. Representative slices of the results of CEE-Alone vs Placebo (light blue) and CEE+MPA vs Placebo (green) on the one standard template.** The detected regions are with threshold of uncorrected  $p < 0.05$ . Red represents the overlap of results between the two methods.

doi:10.1371/journal.pone.0150834.g004

demonstrated significant regions of HT-associated reductions in brain volume, providing further insights into our understanding of the neurobiological underpinnings of HT effects.

A widespread pattern of significant volume loss was detected in women undergoing HT treatments mainly in the anterior cingulate and the adjacent medial frontal gyrus, and the orbitofrontal cortex. Both anterior cingulate and orbitofrontal cortex are key components of the rostral limbic system [39, 40], which are part of a neural circuit consisting of the anterior component of the limbic system. These structures interface with limbic, executive, and behavioral structures that are involved in the motivational evaluation of stimuli. The two regions and their dense connections are associated with higher-level functions such as decision-making [41, 42, 43] and emotional regulation [44, 45]. The anterior cingulate cortex in particular is involved in the ongoing information processing of cognitive resource allocation [46, 47], that is, “cognitive control” [48]. Impairment of the anterior cingulate cortex and the orbitofrontal cortex has been identified in patients with various types of dementia, including frontotemporal dementia [40, 49], vascular dementia [50, 51] and an agitation subgroup [52] of Alzheimer’s disease (AD).

Temporal lobe structures showing HT-associated adverse effects at the trend level include hippocampus, parahippocampal gyrus, inferior temporal gyrus, and the middle temporal gyrus. The integrity of temporal lobe structures, especially those in the medial aspect of the temporal lobe, are critical to the maintenance of memory function. Medial temporal regions are the earliest to show the neurofibrillary tangle pathology of AD [53, 54] which then spreads to adjacent neocortical areas.

Our current findings are consistent with HT-associated GM reductions demonstrated in our previous WHIMS-MRI studies based on region of interest analysis [5]. In our earlier report, we showed that CEE, with or without MPA, was associated with small but significant decrements in hippocampal and frontal regions. However, our study have provided more accurate localizations of brain volume changes and more refined significance levels across regions, by leveraging on the voxel-wise analysis and multiple comparisons. A follow-up pattern classification analysis [55] selected the most discriminative regions for the classification task and identified associations between CEE-Alone therapy and smaller regional volumes, including inferior temporal gyrus and vicinities of the hippocampus, including the perirhinal cortex and the entorhinal cortex. Moreover, our finding of the adverse effect of HT on brain volume is consistent with a VBM study on a different dataset [11]: in an observational study comparing HT users versus nonusers, Lord and colleagues demonstrated reductions in hippocampal and parahippocampal gyrus volumes in HT users.

In contrast to our findings of multiple regions of HT-associated volume reductions, we found no significant regions where HT was associated with larger volumes compared to placebo. However, at the trend level we found larger volumes in the HT group for the posterior cingulate cortical (PCC) area, including the precuneus and the adjacent calcarine fissure. The PCC/precuneus is a key part of the default mode network [56], which is thought to be important for self-referential [57] and episodic memory [58]. Our findings regarding the PCC area are partially in accordance with the results of the previous studies. An early VBM study comparing HT users versus nonusers [10] identified the posterior cingulate gyrus as a region exhibiting larger volumes among younger estrogen users—women around 50 years old. The pattern classification based study of WHIMS on CEE-Alone versus placebo [55] also identified parietal lobe regions where the CEE group had slightly larger volumes. Further a functional MRI study [59] reported higher posterior cingulate activation in hormone users compared with nonusers during a visual working memory task.

The CEE-Alone and CEE+MPA groups, although compared with different placebo controls, demonstrated similar effects of hormone therapy according to the spatial patterns of structural

changes. In Fig 4, we overlaid the results of CEE-Alone and CEE+MPA groups in a single standard template, highlighting regions where the two HT groups share similar structural differences in association with the different interventions. This overlap was most evident in the prefrontal and hippocampal regions, indicating regions of HT-associated GM volume reductions, and in the PCC area which showed higher GM volume in the HT compared with placebo groups. These regions of overlap were consistent with our overall analysis comparing HT vs. placebo, which combined women across both the CEE-Alone and CEE+MPA trials.

Taken together, the most robust findings in our study, which survived more stringent statistical correction, primarily revealed the adverse effect of HT on GM volumes and risk for cognitive impairment and dementia in older women, consistent with prior literature [1, 2, 3, 4, 5, 11, 55, 60, 61, 62]. However, other studies have reported beneficial effects of HT. Two VBM studies [9, 10] indicated higher GM volume in HT users compared with nonusers, which were found widely across the brain gray matter surface. In addition, a few functional neuroimaging studies [59, 63, 64] have also demonstrated that HT can play neuroprotective effects against aging or cognitive decline. However, the majority of studies demonstrating benefits are based on observational studies or studies in younger postmenopausal women. Discrepancies may reflect different experimental strategies and methods used in these studies, as well as differences in the timing of initiation with respect to age and/or the menopausal transition. It should be noted that most studies showing the neuroprotective effects enrolled younger women for their experiments and may reflect a critical window for HT action [65, 66, 67].

Our study involves multiple sites, as most large scale clinical trials do. We promoted standardization across different sites using the ACR phantom QC protocols. The phantom tests have been performed based on a series of measurements, including geometric accuracy, low contrast detectability, high contrast spatial resolution, slice thickness, ghosting artifacts, and more. This phantom test procedure has been a useful method to evaluate the performance of the MRI system, and to determine whether corrective actions are successful. For example, the geometric accuracy test can help to identify gradient mis-calibration and too-low acquisition bandwidth. In addition, after image acquisition, we used the general linear regression model (GLM) as a preprocessing step to further remove the effects of the different clinical sites. Dispersion [68] of different sites can be defined as follows: first, we calculate the sample mean of the whole GM/WM volume values for each site. Next, we calculated the measures of dispersion according to a number of statistics on the sample means, resulting in interquartile range (IQR), mean absolute deviation (MAD), range, and standard deviation (STD). S1 Fig demonstrated the measures of dispersion of different sites, calculated before and after removing the site effects respectively. As shown, the covariance correction has reduced the dispersion of different sites.

Our future work aims to investigate the use of our optimally-discriminative voxel-based morphometric method to study the rate of decline in brain volumes during 4.7 years between the initial and follow-up [69] WHIMS-MRI studies, and also to examine whether the effect of HT on rate of decline differs depending on specific vulnerabilities, e.g. low cognitive function, increased vascular risk, and diabetes.

## Supporting Information

**S1 Fig.** Measures of dispersion of different sites, calculated based on the sample means of the whole A) GM and B) WM volume values.  
(DOCX)

**S1 Table.** The results of GM volume comparisons between HT groups and Placebo, obtained with uncorrected *p* value. *N* denotes the number of significant voxels in each

**anatomical region.  $t$  denotes the  $t$  value calculated.**  
(DOCX)

**S2 Table. The results of WM volume comparisons between HT groups and Placebo, obtained with uncorrected  $p$  value.  $N$  denotes the number of significant voxels in each anatomical region.  $t$  denotes the  $t$  value calculated.**

(DOCX)

## Acknowledgments

The WHI program is funded by the National Heart, Lung, and Blood Institute, National Institutes of Health, U.S. Department of Health and Human Services through contracts HHSN268201100046C, HHSN268201100001C, HHSN268201100002C, HHSN268201100003C, HHSN268201100004C, and HHSN271201100004C. TZ and CD were supported by NIH grant R01AG14971.

A short list of WHI investigators is as follows—**Program Office:** (National Heart, Lung, and Blood Institute, Bethesda, Maryland) Jacques Rossouw, Shari Ludlam, Dale Burwen, Joan McGowan, Leslie Ford, and Nancy Geller; **Clinical Coordinating Center:** (Fred Hutchinson Cancer, Research Center, Seattle, WA) Garnet Anderson, Ross Prentice, Andrea LaCroix, and Charles Kooperberg; **Investigators and Academic Centers:** (Brigham and Women's Hospital, Harvard Medical School, Boston, MA) JoAnn E. Manson; (MedStar Health Research Institute/Howard University, Washington, DC) Barbara V. Howard; (Stanford Prevention Research Center, Stanford, CA) Marcia L. Stefanick; (The Ohio State University, Columbus, OH) Rebecca Jackson; (University of Arizona, Tucson/Phoenix, AZ) Cynthia A. Thomson; (University at Buffalo, Buffalo, NY) Jean Wactawski-Wende; (University of Florida, Gainesville/Jacksonville, FL) Marian Limacher; (University of Iowa, Iowa City/Davenport, IA) Robert Wallace; (University of Pittsburgh, Pittsburgh, PA) Lewis Kuller; (Wake Forest University School of Medicine, Winston-Salem, NC) Sally Shumaker; and **Women's Health Initiative Memory Study:** (Wake Forest University School of Medicine, Winston-Salem, NC) Sally Shumaker.

## Author Contributions

Conceived and designed the experiments: TZ RC SMR MAE CD. Performed the experiments: TZ RC SMR MAE CD. Analyzed the data: TZ RC SMR JEM LDB CBP LHK RNB MAE CD. Wrote the paper: TZ RC SMR JEM LDB CBP LHK RNB MAE CD.

## References

1. Shumaker S, Legault C, Rapp S, Thal L, Wallace RB, Ockene JK, et al. The effects of estrogen plus progestin on the incidence of dementia and mild cognitive impairment in postmenopausal women: The Women's Health Initiative Memory Study (WHIMS). *JAMA* 2003; 289:2663–74.
2. Shumaker SA, Legault C, Kuller L, Rapp SR, Thal L, Lane DS, et al. Conjugated equine estrogens and incidence of probable dementia and mild cognitive impairment in postmenopausal women. *JAMA* 2004; 291:2947–2958. PMID: [15213206](#)
3. Rapp S, Espeland MA, Shumaker SA, Henderson VW, Brunner RL, Manson JE, et al. Effect of estrogen plus progestin on global cognitive function in postmenopausal women: Women's Health Initiative Memory Study. *JAMA* 2003; 289:2663–72. PMID: [12771113](#)
4. Espeland MA, Rapp SR, Shumaker SA, Brunner R, Manson JE, Sherwin BB, et al. Conjugated equine estrogens on global cognitive function in postmenopausal women. *JAMA* 2004; 291:2959–69. PMID: [15213207](#)
5. Resnick SM, Espeland MA, Jaramillo SA, Hirsch C, Stefanick ML, Murray AM, et al. Postmenopausal hormone therapy and regional brain volumes: The WHIMS-MRI Study. *Neurology*. 2009; 72(2):135–142. doi: [10.1212/01.wnl.0000339037.76336.cf](#) PMID: [19139364](#)

6. Ashburner J, Friston KJ. Voxel-based morphometry—the methods. *Neuroimage*. 2000; 11:805–821. PMID: [10860804](#)
7. Good CD, Johnsrude IS, Ashburner J, Henson RN, Friston KJ, Frackowiak RS. A voxel-based morphometric study of ageing in 465 normal adult human brains. *Neuroimage*. 2001; 14:21–36. PMID: [11525331](#)
8. Davatzikos C, Genc A, Xu D, Resnick SM. Voxel-based morphometry using the RAVENS maps: methods and validation using simulated longitudinal atrophy. *Neuroimage*. 2001; 14:1361–1369. PMID: [11707092](#)
9. Erickson KI, Colcombe SJ, Raz N, Korol DL, Scaif P, Webb A, et al. Selective sparing of brain tissue in postmenopausal women receiving hormone replacement therapy. *Neurobiol Aging*. 2005; 26(8):1205–1213. PMID: [15917105](#)
10. Boccardi M, Ghidoni R, Govoni S, Testa C, Benussi L, Bonetti M, et al. Effects of hormone therapy on brain morphology of healthy postmenopausal women: a Voxel-based morphometry study. *Menopause*. 2006; 13(4):584–591. PMID: [16837880](#)
11. Lord C, Engert V, Lupien SJ, Pruessner JC. Effect of sex and estrogen therapy on the aging brain: a voxel-based morphometry study. *Menopause*. 2010; 17(4):846–851. doi: [10.1097/gme.0b013e3181e06b83](#) PMID: [20616671](#)
12. Friston KJ, Holmes AP, Worsley KJ, Poline JP, Frith CD, Frackowiak RS. Statistical parametric maps in functional imaging: a general linear approach. *Hum Brain Mapp*. 1994; 2(4):189–210.
13. Davatzikos C. Why voxel-based morphometric analysis should be used with great caution when characterizing group differences. *Neuroimage*. 2004; 23(1):17–20. PMID: [15325347](#)
14. Jones DK, Symms MR, Cercignani M, Howard RJ. The effect of filter size on VBM analyses of DT-MRI data. *Neuroimage*. 2005; 26(2):546–554. PMID: [15907311](#)
15. Zhang Y, Zou P, Mulhern RK, Butler RW, Laningham FH, Ogg RJ. Brain structural abnormalities in survivors of pediatric posterior fossa brain tumors: a voxel-based morphometry study using free-form deformation. *Neuroimage*. 2008; 42(1):218–229. doi: [10.1016/j.neuroimage.2008.04.181](#) PMID: [18539046](#)
16. Kamitani Y, Sawahata Y. Spatial smoothing hurts localization but not information: pitfalls for brain mappers. *Neuroimage*. 2010; 49:1949–1952. doi: [10.1016/j.neuroimage.2009.06.040](#) PMID: [19559797](#)
17. Zhang T, Davatzikos C. ODVBA: Optimally-Discriminative Voxel Based Analysis. *IEEE Trans Med Imaging*. 2011; 30:1441–1454. doi: [10.1109/TMI.2011.2114362](#) PMID: [21324774](#)
18. Zhang T, Davatzikos C. Optimally-Discriminative Voxel-Based Morphometry significantly increases the ability to detect group differences in schizophrenia mild cognitive impairment and Alzheimer's disease. *Neuroimage*. 2013; 79:94–110. doi: [10.1016/j.neuroimage.2013.04.063](#) PMID: [23631985](#)
19. Zhang T, Koutsouleris N, Meisenzahl E, Davatzikos C. Heterogeneity of Structural Brain Changes in Subtypes of Schizophrenia Revealed Using Magnetic Resonance Imaging Pattern Analysis. *Schizophr Bull*. 2015; 41(1):74–84. doi: [10.1093/schbul/sbu136](#) PMID: [25261565](#)
20. Chaim TM, Zhang T, Zanetti MV, da Silva MA, Louzã MR, Doshi J, et al. Multimodal Magnetic Resonance Imaging Study of Treatment-Naïve Adults with Attention-Deficit/Hyperactivity Disorder. *PIOS ONE*. 2014; 9(10):e110199. doi: [10.1371/journal.pone.0110199](#) PMID: [25310815](#)
21. Erus G, Battapady H, Zhang T, Lovato J, Miller ME, Williamson JD et al. Spatial Patterns of Structural Brain Changes in Type 2 Diabetic Patients and Their Longitudinal Progression With Intensive Control of Blood Glucose. *Diabetes care*. 2015; 38(1):97–104. doi: [10.2337/dc14-1196](#) PMID: [25336747](#)
22. Shumaker SA, Reboussin BA, Espeland MA, Rapp SR, McBee WL, Dailey M, et al. The Women's Health Initiative Memory Study (WHIMS): a trial of the effect of estrogen therapy in preventing and slowing the progression of dementia. *Control Clin Trials*. 1998; 19:604–621. PMID: [9875839](#)
23. Jaramillo SA, Felton D, Andrews L, Desiderio L, Hallam RK, Jackson SD, et al. Women's Health Initiative Memory Study Research Group. Enrollment in a brain magnetic resonance study: results from the Women's Health Initiative Memory Study Magnetic Resonance Imaging Study (WHIMS-MRI) *Acad Radiol*. 2007; 14:603–612.
24. American College of Radiology. Phantom test guidance for the ACR MRI Accreditation Program. Reston, Va: ACR. 1998.
25. Coker LH, Hogan PE, Bryan NR, Kuller LH, Margolis KL, Bettermann K, et al, for the Women's Health Initiative Memory Study. Postmenopausal hormone therapy and subclinical cerebrovascular disease: the WHIMS-MRI Study. *Neurology*. 2009; 72:125–134. doi: [10.1212/01.wnl.0000339036.88842.9e](#) PMID: [19139363](#)
26. Smith SM. Fast robust automated brain extraction. *Hum Brain Mapp*. 2002; 17:143–55. PMID: [12391568](#)

27. Pham DL, Prince JL. Adaptive fuzzy segmentation of magnetic resonance images. *IEEE Trans Med. Imag.* 1999; 18(9):737–752.
28. Kabani NJ, Collins DL, Evans AC. A 3D neuroanatomical atlas. Fourth International Conference on Functional Mapping of the Human Brain, 1998.
29. Shen D, Davatzikos C. HAMMER: hierarchical attribute matching mechanism for elastic registration. *IEEE Trans Med Imaging.* 2002; 21:1421–1439. PMID: [12575879](#)
30. Kiebel SJ, Holmes AP. The general linear model. Academic Press; 2003.
31. Nichols TE, Holmes AP. Nonparametric permutation tests for functional neuroimaging: a primer with examples. *Hum Brain Mapp.* 2002; 15:1–25. PMID: [11747097](#)
32. Hayasaka S, Nichols TE. Validating cluster size inference: random field and permutation methods. *Neuroimage.* 2003; 20:2343–2356. PMID: [14683734](#)
33. Stelzer J, Chen Y, Turner R. Statistical inference and multiple testing correction in classification-based multi-voxel pattern analysis (MVPA): random permutations and cluster size control. *Neuroimage.* 2013; 65:69–82. doi: [10.1016/j.neuroimage.2012.09.063](#) PMID: [23041526](#)
34. Genovese CR, Lazar NA, Nichols T. Thresholding of statistical maps in functional neuroimaging using the false discovery rate. *Neuroimage.* 2002; 15(4):870–878. PMID: [11906227](#)
35. Nichols TE, Hayasaka S. Controlling the familywise error rate in functional neuroimaging: a comparative review. *Stat Methods Med Res.* 2003; 12 (5):419–446. PMID: [14599004](#)
36. Tzourio-Mazoyer N, Landeau B, Papathanassiou D, Crivello F, Etard O, Delcroix N, et al. Automated anatomical labeling of activations in GLM using a macroscopic anatomical arcellation of the MNI MRI single-subject brain. *Neuroimage.* 2002; 15:273–289. PMID: [11771995](#)
37. Talairach J, Tournoux P. Co-planar stereotaxic atlas of the human brain. 3-Dimensional proportional system: an approach to cerebral imaging. 1988.
38. Saltelli A. Sensitivity analysis for importance assessment. *Risk Analysis.* 2002; 22(3):579–90. PMID: [12088235](#)
39. Devinsky O, Morrell MJ, Vogt BA. Contributions of anterior cingulate cortex to behaviour. *Brain.* 1995; 118:279–306. PMID: [7895011](#)
40. Boccardi M, Sabatoli F, Laakso MP, Testa C, Rossi R, Beltramello A, et al. Frontotemporal dementia as a neural system disease. *Neurobiol Aging.* 2005; 26(1):37–44. PMID: [15585344](#)
41. Bechara A, Tranel D, Damasio H. Characterization of the decision-making deficit of patients with ventromedial prefrontal cortex lesions. *Brain.* 2000; 123 (Pt 11):2189–2202. PMID: [11050020](#)
42. Gehring WJ, Willoughby AR. The medial frontal cortex and the rapid processing of monetary gains and losses. *Science.* 2002; 295:2279–2282. PMID: [11910116](#)
43. Kolling N, Behrens TE, Mars RB, Rushworth MF. Neural mechanisms of foraging *Science.* 2012; 336:95–98. doi: [10.1126/science.1216930](#) PMID: [22491854](#)
44. Decety J, Michalska KJ, Kinzler KD. The contribution of emotion and cognition to moral sensitivity: A neurodevelopmental study. *Cerebral Cortex.* 2012; 22(1):209–220. doi: [10.1093/cercor/bhr111](#) PMID: [21616985](#)
45. Hakamata Y, Iwase M, Kato T, Senda K, Inada T. The neural correlates of mindful awareness: a possible buffering effect on anxiety-related reduction in subgenual anterior cingulate cortex activity. *PLOS ONE.* 2013; 8:e75526. doi: [10.1371/journal.pone.0075526](#) PMID: [24130715](#)
46. Botvinick M, Nystrom LE, Fissell K, Carter CS, Cohen JD. Conflict monitoring versus selection-for-action in anterior cingulate. *Nature.* 1999; 402: 179–81. PMID: [10647008](#)
47. Paus T. Primate anterior cingulate cortex: where motor control, drive and cognition interface. *Nat Rev Neurosci* 2001; 2: 417–24. PMID: [11389475](#)
48. Fellows LK, Farah MJ. Is anterior cingulate cortex necessary for cognitive control? *Brain.* 2005; 128 (4):788–796.
49. Rosen HJ, Gorno-Tempini ML, Goldman WP, Perry RJ, Schuff N, Weiner M, et al. Patterns of brain atrophy in frontotemporal dementia and semantic dementia. *Neurology.* 2002; 58:198–208 PMID: [11805245](#)
50. Swartz RH, Stuss DT, Gao F, Black SE. Independent cognitive effects of atrophy and diffuse subcortical and thalamico-cortical cerebrovascular disease in dementia. *Stroke* 2008; 39:822–30. doi: [10.1161/STROKEAHA.107.491936](#) PMID: [18258840](#)
51. Ihara M, Polvikoski TM, Hall R, Slade JY, Perry RH, Oakley AE, et al. Quantification of myelin loss in frontal lobe white matter in vascular dementia, Alzheimer's disease, and dementia with Lewy bodies. *Acta Neuropathol.* 2010; 119: 579–89. doi: [10.1007/s00401-009-0635-8](#) PMID: [20091409](#)

52. Tekin S, Mega MS, Masterman D, Chow T, Garakian J, Vinters HV, et al. Orbitofrontal and anterior cingulate cortex neurofibrillary tangle burden is associated with agitation in Alzheimer disease. *Ann Neurol* 2001; 49:355–361. PMID: [11261510](#)
53. Braak H, Braak E. Neuropathological staging of Alzheimer-related changes. *Acta neuropathologica*. 1991; 82(4):239–259.
54. Delacourte A, David JP, Sergeant N, Buee L, Wattez A, Vermersch P, et al. The biochemical pathway of neurofibrillary degeneration in aging and Alzheimer's disease. *Neurology*, 1999; 52(6):1158–1158. PMID: [10214737](#)
55. Casanova R, Espeland MA, Goveas JS, Davatzikos C, Gaussoin SA, Maldjian JA, et al. Application of machine learning methods to describe the effects of conjugated equine estrogens therapy on region-specific brain volumes. *Magnetic resonance imaging*. 2011; 29(4):546–553. doi: [10.1016/j.mri.2010.12.001](#) PMID: [21292420](#)
56. Raichle ME, MacLeod AM, Snyder AZ, Powers WJ, Gusnard DA, Shulman GL. A default mode of brain function. *Proc Natl Acad Sci USA*. 2001; 98:676–682. PMID: [11209064](#)
57. Kjaer TW, Nowak M, Lou HC. Reflective self-awareness and conscious states: PET evidence for a common midline parietofrontal core. *Neuroimage*. 2002; 17(2):1080–1086. PMID: [12377180](#)
58. Lundstrom BN, Petersson KM, Andersson J, Johansson M, Fransson P, Ingvar M. Isolating the retrieval of imagined pictures during episodic memory: activation of the left precuneus and left prefrontal cortex. *Neuroimage*. 2003; 20(4):1934–1943. PMID: [14683699](#)
59. Berent-Spillon A, Persad CC, Love T, Tkaczyk A, Wang H, Reame NK, et al. Early menopausal hormone use influences brain regions used for visual working memory. *Menopause*. 2010; 17(4):692. doi: [10.1097/gme.0b013e3181cc49e9](#) PMID: [20300040](#)
60. Grady D, Yaffe K, Kristof M, Lin F, Richards C, Barrett-Connor E. Effect of postmenopausal hormone therapy on cognitive function: the Heart and Estrogen/Progestin Replacement Study. *Am J Med* 2002; 113:543–548. PMID: [12459399](#)
61. Espeland MA, Brunner RL, Hogan PE, Rapp SR, Coker LH, Legault C, et al. Long-Term Effects of Conjugated Equine Estrogen Therapies on Domain-Specific Cognitive Function: Results from the Women's Health Initiative Study of Cognitive Aging Extension. *J Am Geriatr Soc*. 2010; 58(7):1263–1271. doi: [10.1111/j.1532-5415.2010.02953.x](#) PMID: [20649689](#)
62. Goveas JS, Espeland MA, Hogan P, Dotson V, Tarima S, Coker LH, et al. Depressive symptoms, brain volumes and subclinical cerebrovascular disease in postmenopausal women: The Women's Health Initiative MRI Study. *J Affect Disord*. 2011; 132(1):275–284.
63. Thomas J, Météreau E, Déchaud H, Pugeat M, Dreher JC. Hormonal treatment increases the response of the reward system at the menopause transition: A counterbalanced randomized placebo-controlled fMRI study. *Psychoneuroendocrinology*. 2014; 50:167–180. doi: [10.1016/j.psyneuen.2014.08.012](#) PMID: [25222702](#)
64. Rasgon NL, Geist CL, Kenna HA, Wroolie TE, Williams KE, Silverman DH. Prospective Randomized Trial to Assess Effects of Continuing Hormone Therapy on Cerebral Function in Postmenopausal Women at Risk for Dementia. *PIOS ONE*. 2014; 9(3):e89095. doi: [10.1371/journal.pone.0089095](#) PMID: [24622517](#)
65. Resnick SM, Henderson VW. Hormone therapy and risk of Alzheimer disease: a critical time. *JAMA*, 2002; 288(17):2170–2172. PMID: [12413378](#)
66. Whitmer RA, Quesenberry CP, Zhou J, Yaffe K. Timing of hormone therapy and dementia: the critical window theory revisited. *Ann Neurol*. 2011; 69(1):163–169. doi: [10.1002/ana.22239](#) PMID: [21280086](#)
67. Maki PM. The Critical Window Hypothesis of Hormone Therapy and Cognition: A Scientific Update on Clinical Studies. *Menopause*. 2013; 20(6):695–709. doi: [10.1097/GME.0b013e3182960cf8](#) PMID: [23715379](#)
68. Natrella, M., NIST/SEMATECH e-handbook of statistical methods. 2010.
69. Coker LH, Espeland MA, Hogan PE, Resnick SM, Bryan RN, Robinson JG, et al. Change in brain and lesion volumes after CEE therapies The WHIMS-MRI studies. *Neurology*. 2014; 82(5):427–34. doi: [10.1212/WNL.000000000000079](#) PMID: [24384646](#)